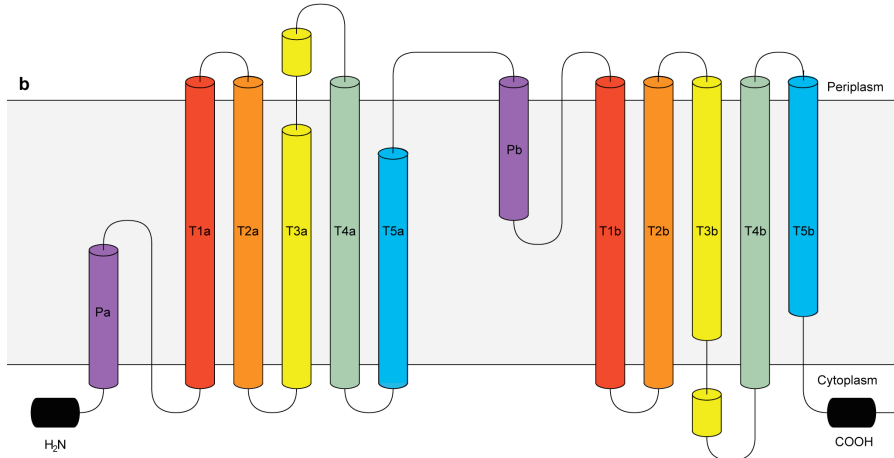
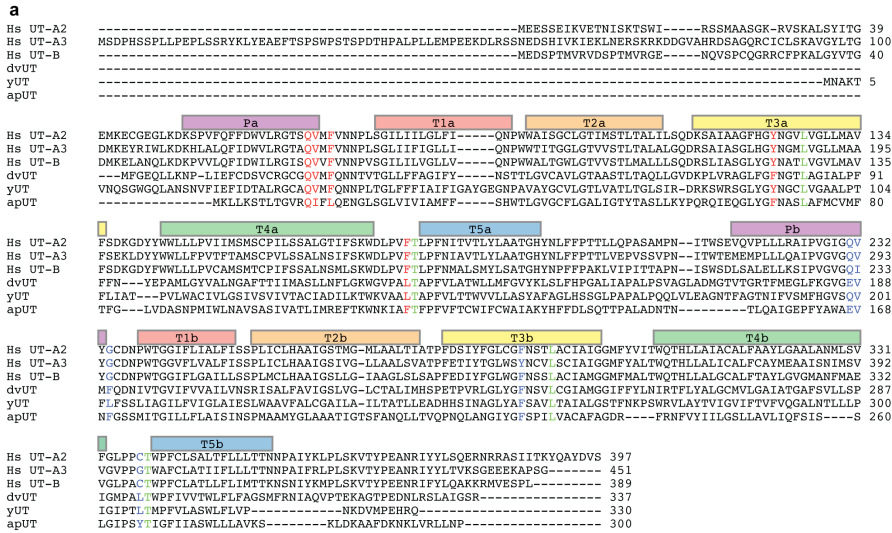


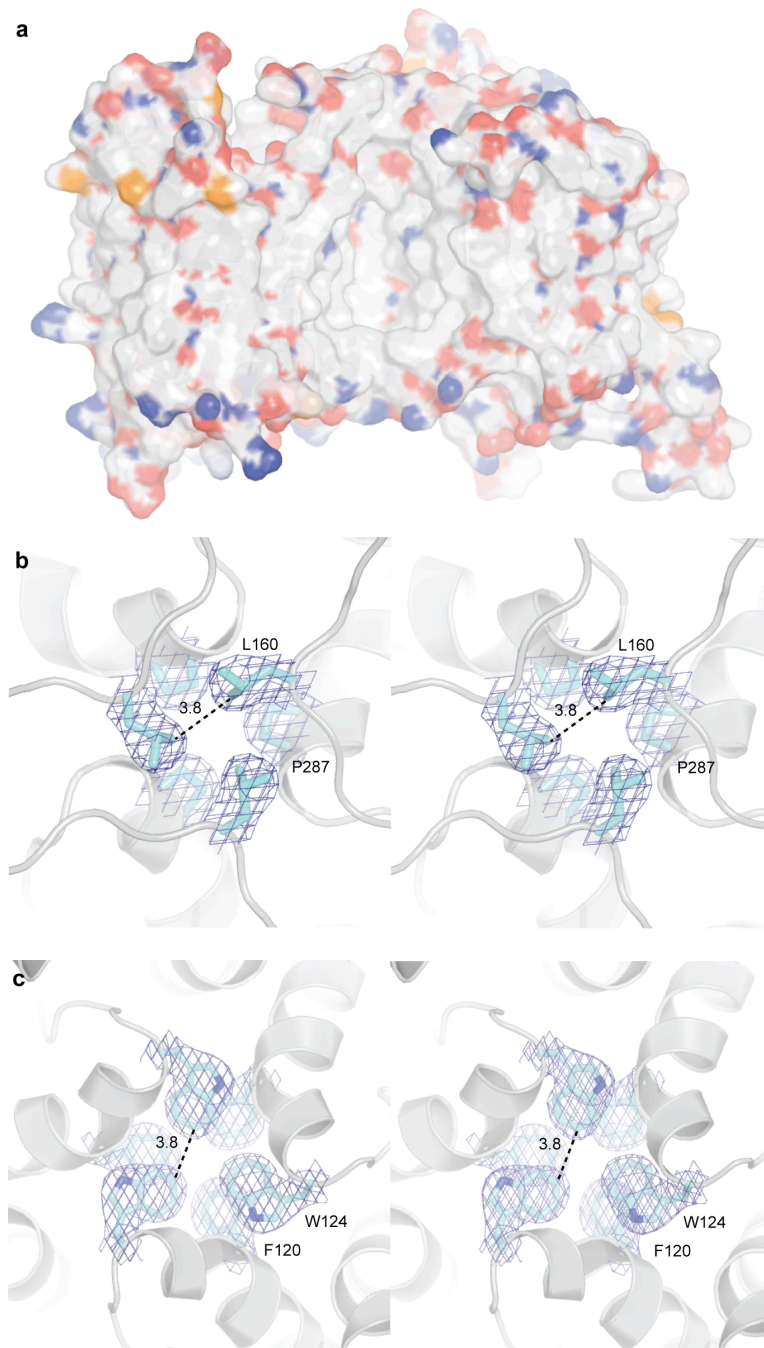
Supplemental Tables and Figures.

Table 1 X-ray refinement statistics

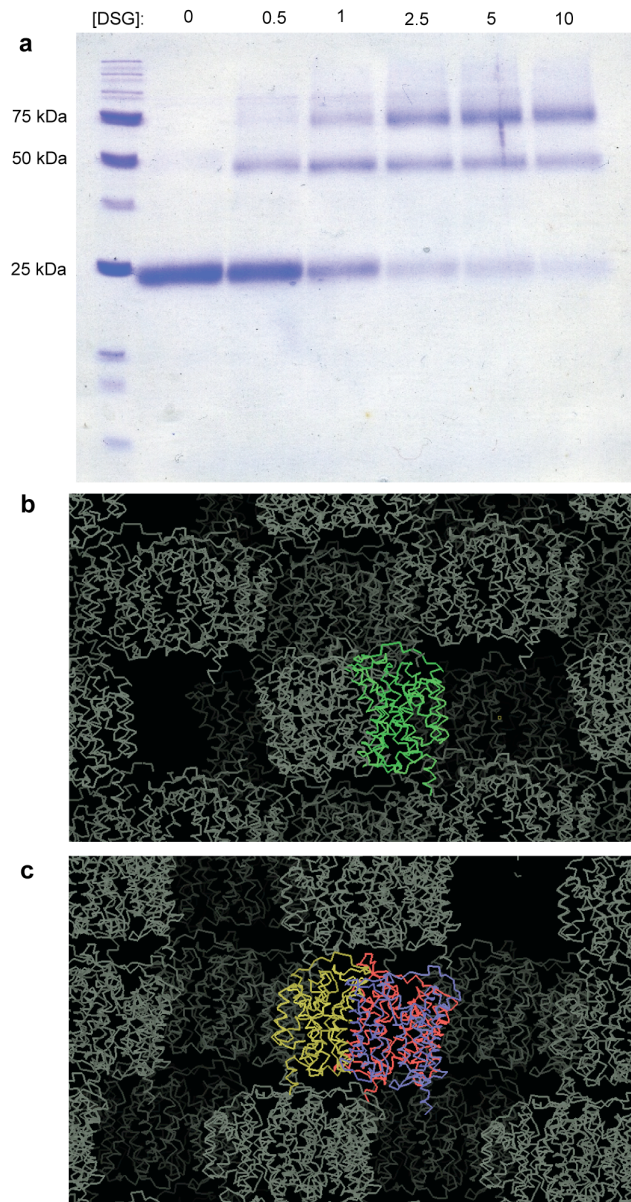
Dataset	Thimerosal	KAu(CN) ₂	KAu(CN) ₂ /DMU
Data Collection and Phasing			
Resolution (Å)	2.5	2.3	2.4
Space group	P6(3)	P6(3)	P6(3)
Unit cell	a=108.92, c=86.60	a=110.13, c=84.86	a=110.11, c=84.87
Number of reflections	20107 (2010)	24536 (1783)	21798 (1573)
Completeness	99.8 (98)	99.2 (95.7)	99.6 (98.3)
I/σ	25.8 (2.5)	20.1 (1.4)	20.1 (1.1)
Rmerge (%)	11.3	8.9	9.1
Figure of Merit	0.4	—	—
Refinement			
<i>R</i> _{work} / <i>R</i> _{free}	—	17.9/20.4	18.6/21.4
Number of atoms			
Protein	—	2485	2482
Ligand/ion	—	9	21
Water	—	55	28
B-factors			
Protein	—	48.2	44.4
Ligand/ion	—	79.4	74.5
Water	—	59.6	60.0
R.m.s deviations			
Bond lengths (Å)	—	0.018	0.015
Bond angles (°)	—	1.47	1.34



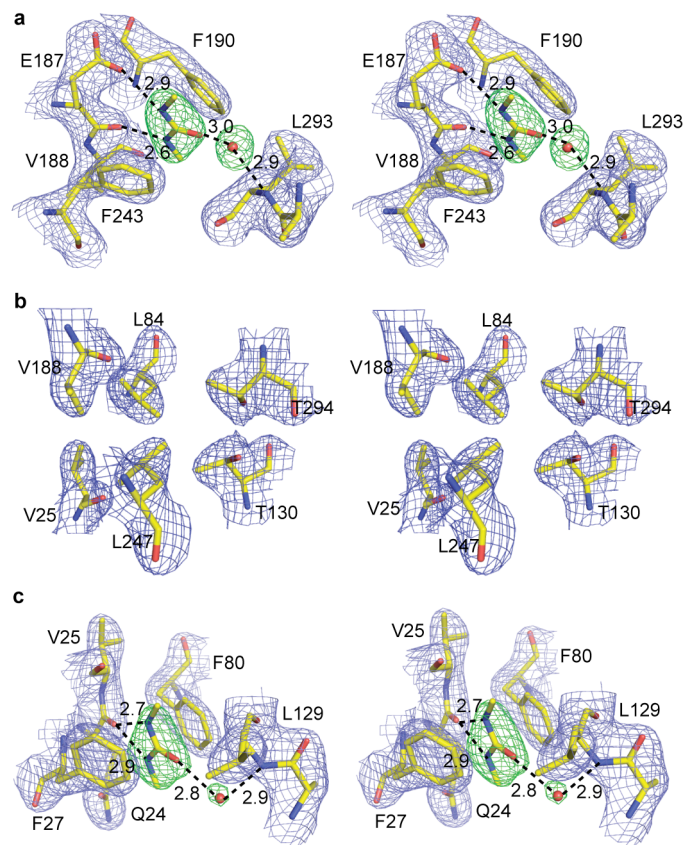
Supplementary Figure 1: Primary structure and topology of dvUT. a. The program ClustalW was used to calculate a multiple sequence alignment of human and bacterial (*Yersinia pseudotuberculosis*, *Actinobacillus pleuropneumoniae*, and *Desulfovibrio vulgarius*) urea transporters. The colored bars correspond to the location of intramembrane helices in the dvUT structure. Colored residues line the selectivity filter, and red, green, and blue corresponds to site S_i , S_m , and S_o , respectively. **b.** Schematic showing the membrane topology of dvUT, with both termini oriented intracellularly. Pairs of homologous helices are colored identically; helices in black are not related.



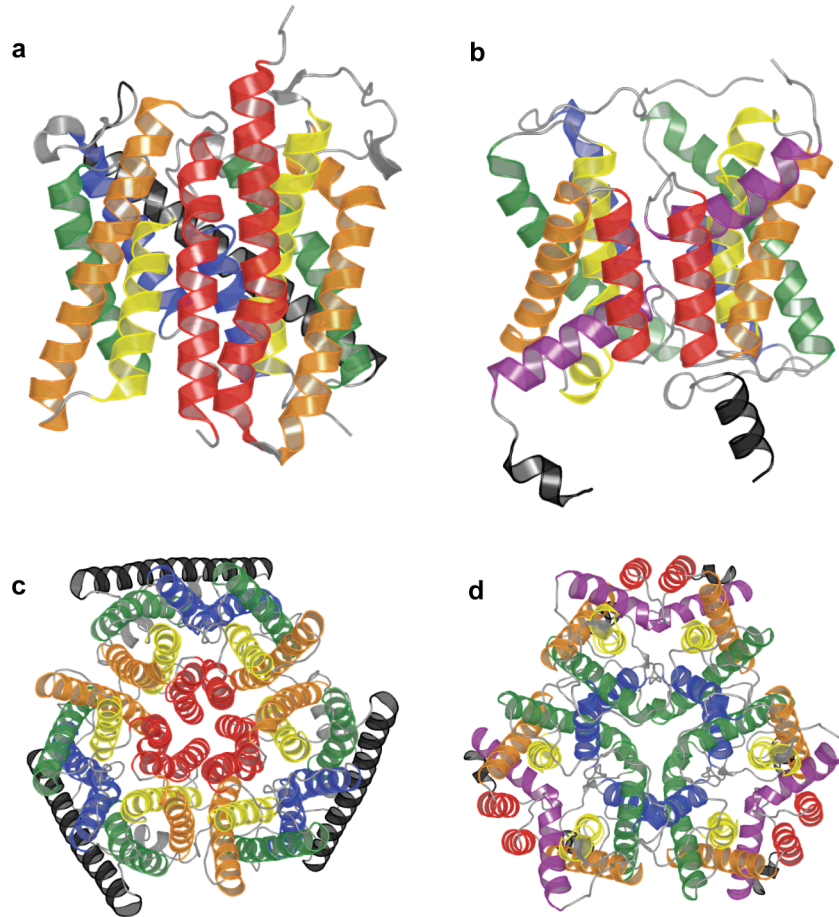
Supplementary Figure 2: Trimer interface of dvUT. **a.** Surface representation of dvUT with one subunit removed to expose the central cavity. **b-c.** Stereo view of residues sealing the central cavity on the periplasmic (**b**) and cytoplasmic (**c**) face of the trimer interface. The dark blue mesh corresponds to the 2Fo-Fc electron density contoured at 1.5σ .



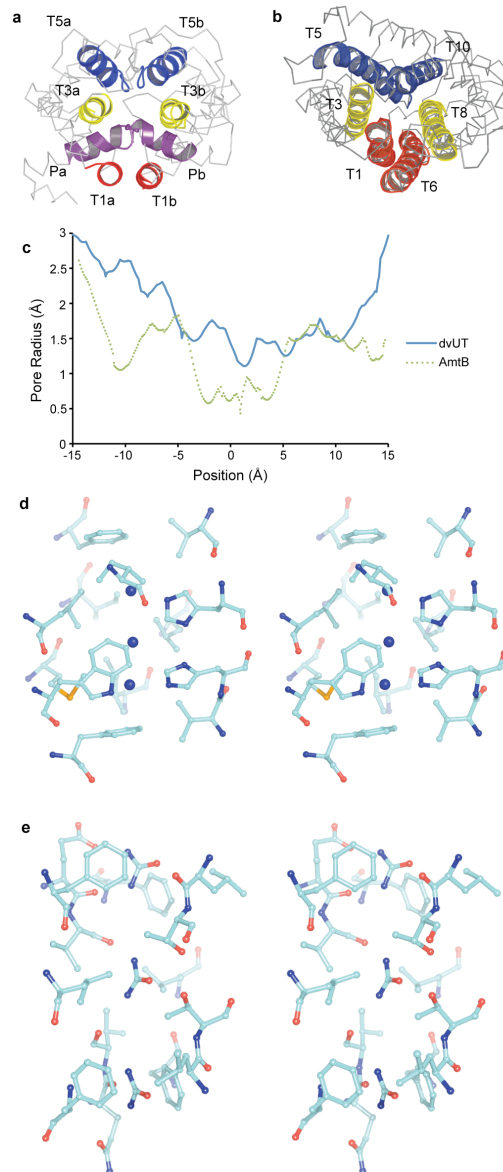
Supplementary Figure 3: Biochemical and crystallographic evidence for the dvUT trimer. **a.** Chemical crosslinking of dvUT. Purified dvUT was incubated with the amine-to-amine crosslinking agent disuccinimidyl glutarate (Pierce) at concentrations varying from 0-10 mM and then run on an SDS-PAGE gel. **b-c.** Crystallographic packing of dvUT in the gold-derivatized P6₃ (**b**) and native P3₁ (**c**) crystal forms. The asymmetric units are shown in color.



Supplementary Figure 4: Stereo view of the dimethylurea binding sites. a-c. Stereo views of the S_o (a), S_m (b) and S_i (c) regions of the selectivity filter for dvUT-dimethyl urea complex. The amino acid residues are shown in stick representation, and covered with 2Fo-Fc electron density map contoured at 1.5σ (dark blue). Green contour lines in the S_o and S_i sites correspond to 3.0σ Fo-Fc electron density calculated with both the dimethylurea and the displayed water molecule omitted.



Supplementary Figure 5: Comparison of the urea and ammonia transporter folds. a-b. Cartoon representations of the AmtB (a, PDB 1U7G) and dvUT (b) protomers. Helices corresponding to the hypothetical five-helix ancestral protein are colored red, orange, yellow, green and blue in both proteins. Helices in black are unrelated. **c-d.** The AmtB (c) and dvUT (d) trimers drawn with the same coloring scheme.



Supplementary Figure 6: Comparison of the dvUT and AmtB selectivity

filters. a-b. The dvUT (a) and AmtB (b) protomers are shown with the pore perpendicular to the plane of the image. Helices involved in forming the pores are colored according to the same scheme as used in Supplemental Figure 5. **c.** Pore radii for dvUT (blue solid line) and AmtB (green dotted line) calculated with the program HOLE (Smart, O.S., Goodfellow, J.M. and Wallace, B.M. *Biophysical Journal* **65**:2455-2460 (1993)). **d-e.** Stereoviews of the central regions of the

AmtB (**d**) and dvUT (**e**) pores. The urea molecules shown modelled in the dvUT pore in (**e**) are proposed locations for potential urea-binding sites.